Heliyon 6 (2020) e05368

Contents lists available at ScienceDirect

Heliyon

journal homepage: www.cell.com/heliyon

Research article

Synthesis and biological properties of a series of aryl alkyl disulfide derivatives

Nausheen Joondan, Marie Agnes Thessa Inassee, Minu Gupta Bhowon, Sabina Jhaumeer Laulloo *

Department of Chemistry, Faculty of Science, University of Mauritius, Reduit, Mauritius

ARTICLE INFO

Keywords:
Organic chemistry
Theoretical chemistry
Pharmaceutical chemistry
Disulfides
Alkyl chain
Antibacterial
CMC
BSA
Molecular docking

ABSTRACT

Disulfide containing compounds are recognized for their wide range of biological properties and are known for their important applications in the pharmaceutical field. In this study, a series of diaryl disulfides with varying alkyl chain length (C_8-C_{16}) was synthesized and assessed for their physicochemical and biological properties. The interactions of compounds with bovine serum albumin (BSA) was investigated in order to study their ability to bind with blood serum protein. An increase in the binding constants (K_a) was observed with increasing chain length C_8-C_{12}, while a decrease in value was obtained with compounds of chain length C_{14} and C_{16} showing a cut off effect at C_{12}. The thermodynamic parameters of binding indicated that the compounds bound to BSA mostly by van der Waals forces and hydrogen bonding. Molecular docking studies showed that the diaryl disulfides displayed greater binding affinity to Trp 213 rather than the Trp 134 residue on the BSA molecule. The trend observed in molecular docking is in line with the fluorescence binding studies whereby the C_{12} derivative was found to show optimum affinity with BSA. The disulfide with chain length C_{10} showed moderate antibacterial activity the highest inhibitory activity against *Bacillus cereus*. The cytotoxicity of the disulfides towards HaCaT cells decreased from C_8 to C_{14}. The overall results obtained show that these disulfides have potent antibacterial properties against Gram-positive bacteria *Bacillus cereus* at concentrations which are relatively non-toxic to normal cells.

1. Introduction

Diaryl disulfides form part of one of the most important and widely used compounds by synthetic chemists and are considered among the most momentous structural motifs in chemistry, possessing important functions in pharmaceutics and biologically active compounds [1, 2, 3]. There are numerous drugs containing disulfide moiety which are being used to treat medical conditions such as diabetes insipidus [4] and T-cell lymphoma [5]. Disulfide likages is important for proteins' functionalization and are being extensively used in the design of controlled drug delivery systems (CDDS) [6, 7].

The development of lead drugs is often base on the introduction of a number of chemical moieties, which produce chemical diversity and influence their properties [8, 9, 10]. Aromatic compounds are well known for their synthetic pathways and for this reason, they are being used extensively in drugs [11, 12]. Long alkyl chains in aryl alkyl systems bearing are known to influence their physicochemical properties. Increase in the length of alkyl chain impacts significantly on the micellization process of molecules by lowering their critical micelle concentration (CMC) values, rendering them more effective in reducing surface water tension [5]. Addition of other functional groups to the aryl disulfide compounds can influence both their chemical and biological properties. For example, amide functionalized molecules are able to form intermolecular hydrogen bonding, causing tighter packing at the air-water interface and at a hydrophobic surface [13].

A number of diaryl disulfide Schiff bases has been demonstrated to act as antibacterial and herbicidal agents [14, 15]. Another disulfide analogue, the bis-chloro-phenyl disulfide has been reported for its effectiveness as potent anticancer agent with specific target the stabilization of the tumor suppressor, programmed cell death 4 (Pdcd4) [16].

Herein, a series of compounds derivatives containing a combination of useful functionalities such as aromatic, amide moiety, disulfide linkage and long alkyl chains are reported. Moreover, in an attempt to fully exploit the potential application of these compounds, an array of

* Corresponding author.
E-mail address: sabina@uom.ac.mu (S. Jhaumeer Laulloo).

https://doi.org/10.1016/j.heliyon.2020.e05368
Received 22 July 2020; Received in revised form 23 August 2020; Accepted 26 October 2020

biological and physicochemical properties including critical micelle concentration (CMC), bovine serum albumin (BSA) binding ability, antibacterial activity as well as their cytotoxicity were investigated.

2. Results and discussion

In an attempt to investigate the influence of hydrophobicity on the physicochemical and biological properties of disulfides, a series of bis-amino phenyl disulfide derivatives with varying alkyl chains (C_8-C_{16}) were synthesized.

2.1. Synthesis

The disulfides 1 to 5 were synthesized in a two-step reaction (Figure 1). Fatty acid chlorides (C_8, C_{10}, C_{12}, C_{14} and C_{16}) prepared in situ were reacted with bis-amino phenyl disulfide in the presence of triethylamine (TEA) and dimethyl amino pyridine (DMAP).

The new band at 1655-1660 cm^{-1} in the IR spectra of 1-5 indicated the successful formation of the amide bond. The amide proton and amide carbonyl appeared at δ 8.36–8.39 ppm and δ 171.4 ppm in the ^{1}H and ^{13}C NMR spectra respectively. The aliphatic protons appeared in the range of δ 0.84–2.14 ppm. The tertiary aromatic carbons were observed at δ 123.3 - δ 123.4 ppm and δ 139.9 ppm respectively. The NMR spectra of the disulfide 3 is shown in the supplementary material (Figure S1, S2, S3 and S4). The assignments of the different protons and carbons were confirmed by 2D NMR (Supplementary material Table S1).

2.2. Critical micelle concentration

In aqueous solutions, compounds possessing long hydrophobic chain are known to form aggregates called micelles. The critical micelle concentration (CMC) is the concentration at which a compound form micelles at a particular temperature, and it is an important solution property which influences the biological activity of the compound. The CMC of the disulfides 1-5 were investigated at 25 °C by fluorescence spectroscopic technique using pyrene as probe (Figure 2).

A decrease in the CMC values of the disulfides was observed from C_8 to C_{16} (Table 1). This is due to the increase in hydrophobic interactions which renders micellar formation more favourable as previously reported [17]. The following Kleven's equation between the CMC values and chain length (n) was obtained for disulfides 1-5 (Eq. (1)) (Figure 3) [18].

$$\log CMC = 0.0599n - 0.2875 \quad (1)$$

2.3. Bovine serum albumin (BSA) binding studies

Serum albumin, the protein found in blood plasma to transport hormones, fatty acids and various compounds through the blood stream. BSA has been used as a model protein for the study of binding ability of bioactive compounds with serum albumin due to its stability and its similarity to human serum albumin (HSA). The measurement of the binding properties of BSA with the disulfides 1 to 5 with BSA was investigated by fluorescence spectroscopy and the effect of hydrophobicity on the binding affinity of the disulfides to BSA was explored.

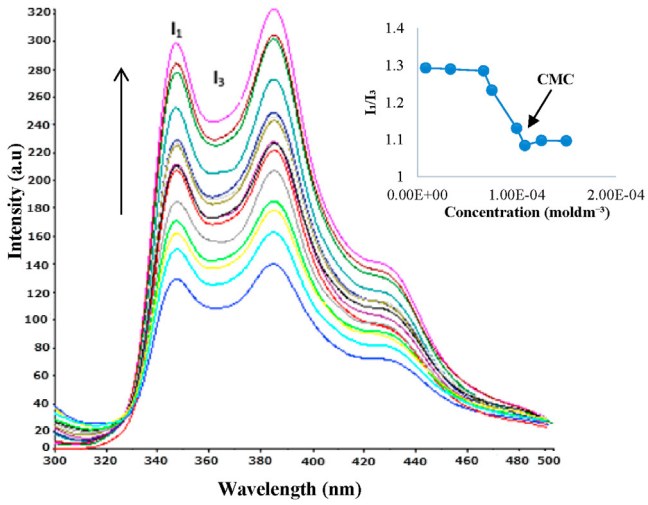

Figure 2. Fluorescence spectrum of pyrene with increasing concentration of disulfide 3. The inset represents the Stern-Volmer plot.

2.3.1. Steady state/intrinsic fluorescence study

Fluorescence spectroscopy can provide information regarding the quenching mechanism, the binding constant and the number of binding sites involved in the binding interaction between plasma protein and a target molecule [19]. Fluorescence quenching can occur either by dynamic mechanism which involves diffusive encounters or by static mechanism which involves complex formation [20]. In order to evaluate the quenching mechanism of the disulfides under investigation, the Stern-Volmer equation (Eq. (2)) was used.

$$F_0/F = 1 + K_q\tau_0\,[Q] = 1 + K_{sv}\,[Q] \quad (2)$$

where F_0: fluorescence intensity of pure BSA; F: fluorescence intensity of BSA in the presence of the disulfide. K_q: bimolecular quenching constant; K_{sv}: Stern-Volmer quenching constant. The value of K_{sv} and K_q gives an overview of the mechanism of binding, i.e either static or dynamic process. [Q] and τ_0 correspond to the concentration of the disulfide and the average lifetime of the pure BSA molecules (10^{-8} s) respectively [21]. For static quenching, Eq. (3) was used.

$$\text{Log}\,[(F_0\text{-}F)/F] = \log K_a + n\log[Q] \quad (3)$$

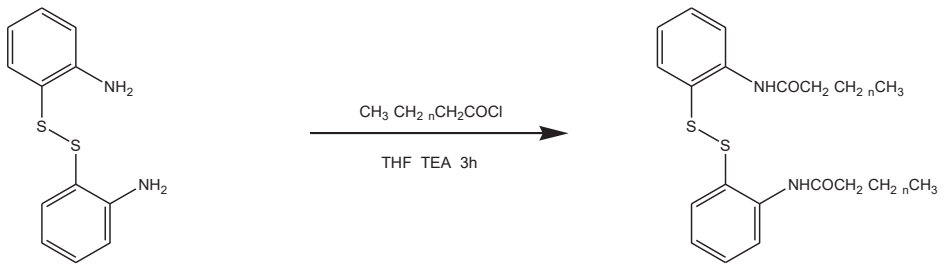

Dioctyl 2 2'-disulfanediyldibenzamide 1 n=5
Didecyl 2 2'-disulfanediyldibenzamide2 n=7
Didodecyl 2 2'-disulfanediyldibenzamide 3 n=9
Dimyristoyl 2 2'-disulfanediyldibenzamide 4 n=11
Dipalmitoyl 2 2'-disulfanediyldibenzamide 5 n=13

Figure 1. Synthesis of compounds 1 to 5.

Table 1. CMC of compounds 1 to 5.

Compound	Chain length	CMC (mM)
1	C_8	0.163
2	C_{10}	0.130
3	C_{12}	0.108
4	C_{14}	0.075
5	C_{16}	0.054

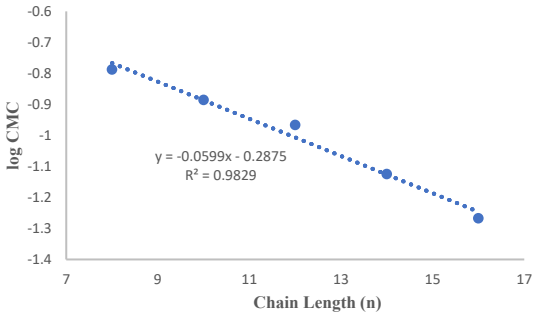

Figure 3. Graph of log CMC v/s Chain length (n).

where K_a (M^{-1}): binding constant; n: number of binding sites.

The intensity of the band was found to decrease markedly with an increase in concentration of disulfides 1-5, suggesting formation of a non-fluorescent complex between the disulfides 1-5 and BSA. However, no shift in wavelength was observed. A static mechanism was proposed for the binding of the disulfides to BSA since the calculated k_q was greater than the scattering collision quenching rate constant (2×10^{10} $M^{-1}s^{-1}$) (Table 2).

The K_a values obtained give an indication about the plasma distribution of the disulfides being studied. Weak binding corresponds to poor distribution of the disulfide, while strong binding is reveals a low plasmatic concentration of the free disulfide [22]. In general, the disulfides 1-5 displayed moderate to high binding constant with BSA (Supplementary material Figure S5). As the carbon chain length increased from C_8-C_{12} (1-3), a corresponding increase in the magnitude of K_a values was obtained. However, a further increase in chain length from C_{12} to C_{16} resulted in a decrease in the K_a values for disulfides 4 and 5. This implies that an increase in hydrophobicity increases the binding strength of the disulfide to BSA from chain length C_8-C_{12}, displaying a cut-off effect at C_{12} after which the binding affinity decreases (Table 3).

2.3.2. Thermodynamic parameters and binding forces

Hydrogen bonding, van der Waals, electrostatic, and hydrophobic interactions are the main forces of attractions that are involved in the binding of small molecules with BSA. These interactions can be described by thermodynamic parameters namely, free energy (ΔG), enthalpy (ΔH) and entropy (ΔS) and hence used to determine the type of binding taking place between the compounds under investigation and BSA. There are 3 sets of conditions for ΔH and ΔS indicating the type of interaction in BSA binding [21]. When $\Delta H > 0$ and $\Delta S > 0$, hydrophobic interactions are the main mode of binding. If $\Delta H < 0$ and $\Delta S > 0$ electrostatic interactions are more prominent and when $\Delta H < 0$ and $\Delta S < 0$, van der Waals and hydrogen bonding are more important.

In order to characterize the binding forces of the disulfides 1 to 5 to BSA, the thermodynamic parameters of binding were determined at 298, 308 and 313 K. The values for ΔH, ΔS and ΔG were calculated using Eqs. (4) and (5)

$$\Delta G = - RT \ln K_a \quad (4)$$

Where T is the absolute temperature, K_a the binding constant at temperature T and R the gas constant. The values of ΔH and ΔS can be analyzed on the basis of the van't Hoff's formula:

$$\ln K_a = -\frac{\Delta H}{RT} + \frac{\Delta S}{R} \quad (5)$$

Where T is the absolute temperature, K_a the binding constant and R the gas constant.

The value of ΔG was then calculated using Eq. (6)

$$\Delta G = \Delta H - T\Delta S \quad (6)$$

From Table 3, it can be observed that for disulfides 1-5 the ΔG values are negative, implying that complex formation with BSA occurs spontaneously at all temperatures. Moreover, the negative values obtained for ΔH and ΔS indicate that the BSA-disulfide interaction is enthalpically driven but entropically unfavorable.

From the sets of conditions mentioned, since the values obtained for ΔH and ΔS are both negative, it can be deduced that interactions between BSA and the disulfides 1-5 occur mainly via van der Waal's forces and hydrogen bonding [21].

2.3.3. Competitive binding experiments using site markers

It is generally known that BSA consists of three main domains (I, II and III), each containing two subdomains A and B. Binding of small molecules to BSA can occur at two main sites namely subdomain IIA (site I) and subdomain IIIA (site II). Warfarin and ibuprofen were used as site markers to represent the binding site I and site II of BSA respectively. They can be used to determine the precise binding site of compounds to BSA by performing competitive binding experiments [23].

To establish the binding sites of the compounds on BSA, binding studies of disulfides 1 to 5 of varying concentrations were investigated in the presence of site markers warfarin and ibuprofen. The binding constants K_a of compounds 1-5 were found to be lower in the presence of both warfarin and ibuprofen suggesting competitive binding of the compounds at both warfarin and ibuprofen binding sites (Table 4). This concludes that disulfides 1-5 bind to BSA molecule at both site I and site II subdomains.

2.4. Molecular docking

From the fluorescence binding studies, disulfide 3 was found to show optimum binding affinity with BSA molecule. Disulfide 3 was constructed and docked in both Trp 213 and Trp 134 region of the BSA molecule. From the ΔG values, it was found that disulfide 3 showed greater binding affinity to the Trp 213 (-17.07 kJ mol^{-1}) over the Trp 134 (-11.91 kJ mol^{-1}) residue. The other disulfide derivatives were then docked around the Trp 213 residue.

Table 2. Values for Stern-Volmer constant (K_{sv}), bimolecular quenching constant (K_q), binding constant (K_a) and number of binding site (n) for 1 to 5.

Disulfide	Chain length	n	K_{sv} x 10^4 (M^{-1})	K_q x 10^{12} ($M^{-1}s^{-1}$)	K_a (M^{-1})
1	C_8	0.76	7.45	7.45	5.47×10^3
2	C_{10}	1.23	2.26	2.26	2.25×10^5
3	C_{12}	1.22	3.16	3.16	5.88×10^8
4	C_{14}	1.27	25.8	25.8	6.89×10^6
5	C_{16}	0.74	1.40	1.40	1.02×10^3

Table 3. Effect of temperature on the binding constant K_a and the thermodynamic parameters (ΔG, ΔH and ΔS) of the interaction of compounds 1 to 5 with BSA.

Compound	Temperature (T) (K)	1/T/x 10^{-3} (K^{-1})	K_a/M^{-1}	ln K_a	ΔG ($KJmol^{-1}$)	ΔH/($KJmol^{-1}$)	ΔS/($Jmol^{-1}K^{-1}$)
1	298	3.356	5.47×10^3	8.61	-21.68	-109.5	-294.7
	308	3.300	3.25×10^3	8.09	-18.73		
	313	3.194	4.61×10^2	6.13	-17.26		
2	298	3.356	2.25×10^5	12.32	-30.60	-325.26	-988.78
	308	3.300	3.58×10^3	8.18	-20.76		
	313	3.194	4.05×10^2	6.00	-15.77		
3	298	3.356	5.88×10^8	20.19	-49.38	-646.07	-2002.29
	308	3.300	4.62×10^4	10.74	-29.36		
	313	3.194	2.79×10^3	7.93	-19.35		
4	298	3.356	6.90×10^6	13.45	-32.08	-84.02	-174.29
	308	3.300	1.14×10^5	11.64	-30.34		
	313	3.194	1.07×10^5	11.58	-29.47		
5	298	3.356	1.02×10^3	6.93	-16.18	-97.23	-271.98
	308	3.300	5.70×10^1	4.04	-13.46		
	313	3.194	2.93×10^2	5.48	-12.10		

ΔH: enthalpy change, ΔS: entropy change, ΔG: free energy.

The disulfides (1-4) showed negative binding free energies (ΔG_{bind}) which indicates spontaneous binding of the disulfides with BSA molecule while positive value for 5 showed that the binding of the compound with BSA is not favourable (Table 5). Disulfide 3 showed greatest binding affinity to BSA molecule, as indicated by a more negative ΔG_{bind} value (-17.07 kJ mol^{-1}). The trend observed in the binding energies obtained from molecular docking was concordant to that observed in the fluorescence binding experiments.

The active site was further analyzed to identify the amino acid residues in BSA that interacted with the disulfides 1-5 (Figure 4). Although disulfides 1-5 were found to bind in close proximity to the Trp 213 residue, no direct interactions (either by hydrogen bonding or hydrophobic interactions) were observed between the compound and Trp 213 residue. The carbonyl group of disulfides 2 and 3 form hydrogen bonds with the ε-NH_2 moiety of the Lys 294 and Lys 211 respectively. The two carbonyl groups of disulfide 4 interact with two NH_2 of the guanidino group of Arg 217 residue while one of the carbonyl group form hydrogen bond with ε-NH_2 moiety of the Lys 294. The long alkyl chains of disulfides 1-4 were found to be well embedded in the binding cavity of BSA, where they interact with BSA residues via hydrophobic interactions. However, only one of the alkyl chains of compound 5 was found to be in the cavity of BSA, while the other chain showed minimal hydrophobic contact with the residues. This might explain for its lower binding affinity for BSA molecule.

Table 4. Binding constants for competitive binding of compounds 1-5 in the presence of ibuprofen and warfarin.

Compound	Site marker	K_a (M^{-1})
1	Blank	5.06×10^3
	Warfarin	4.95×10^3
	Ibuprofen	2.11×10^3
2	Blank	4.29×10^5
	Warfarin	1.57×10^4
	Ibuprofen	6.46×10^4
3	Blank	1.06×10^9
	Warfarin	1.03×10^7
	Ibuprofen	5.24×10^7
4	Blank	3.83×10^6
	Warfarin	3.42×10^5
	Ibuprofen	3.10×10^4
5	Blank	1.79×10^5
	Warfarin	3.83×10^3
	Ibuprofen	3.55×10^3

2.5. Antibacterial activity

The disulfides 1-5 exhibit moderate antibacterial activity against the Gram-positive bacteria tested. The MIC values obtained against *S. aureus* decreases from C_8 to C_{12} and then increases up to a chain of C_{16}, showing an increase in antibacterial activity with a cut-off point at C_{12} (Table 6). In the case of *B. cereus*, the cut-off point was observed at C_{10}. The disulfides were less active against the three Gram-negative strains tested and this might be due to the additional membrane of lipopolysaccharides generally present in Gram-negative bacteria which render the strains more resistant to antimicrobial agents. Among the derivatives tested, disulfide 2 (C_{10}) exhibits the highest inhibitory activity against *B. cereus* with an MIC value of 2.53 mM.

2.6. Cytotoxicity studies

In an attempt to evaluate their cytotoxic potential of the derivatives, the disulfides 1-4 were tested using the MTT assay on the immortalized non-tumorigenic human epidermal (HaCaT) cell line. Due to poor solubility, the disulfide 5 was not analysed. Based solely on the changes in cell morphology, a considerable amount of cell death was observed when the HaCaT cells were treated with disulfide 1 compared to disulfide 3, indicating that disulfide 1 exhibits higher cytotoxicity towards the HaCaT cells (Figure 5).

As the concentration of disulfides 1 and 3 increases from 2.5 mg/mL to 20 mg/mL, an overall increase in cell death was observed. Disulfide 4 were found to be non-cytotoxic at the different concentration tested (Table 7).

The % cell viability was evaluated using Eq. (7):

Table 5. Binding free energies (ΔG_{bind}) of the compounds in the Trp-213 binding site.

Compound	ΔG_{bind} (kJ mol^{-1})
1	-16.15
2	-16.23
3	-17.07
4	-13.60
5	+2.00

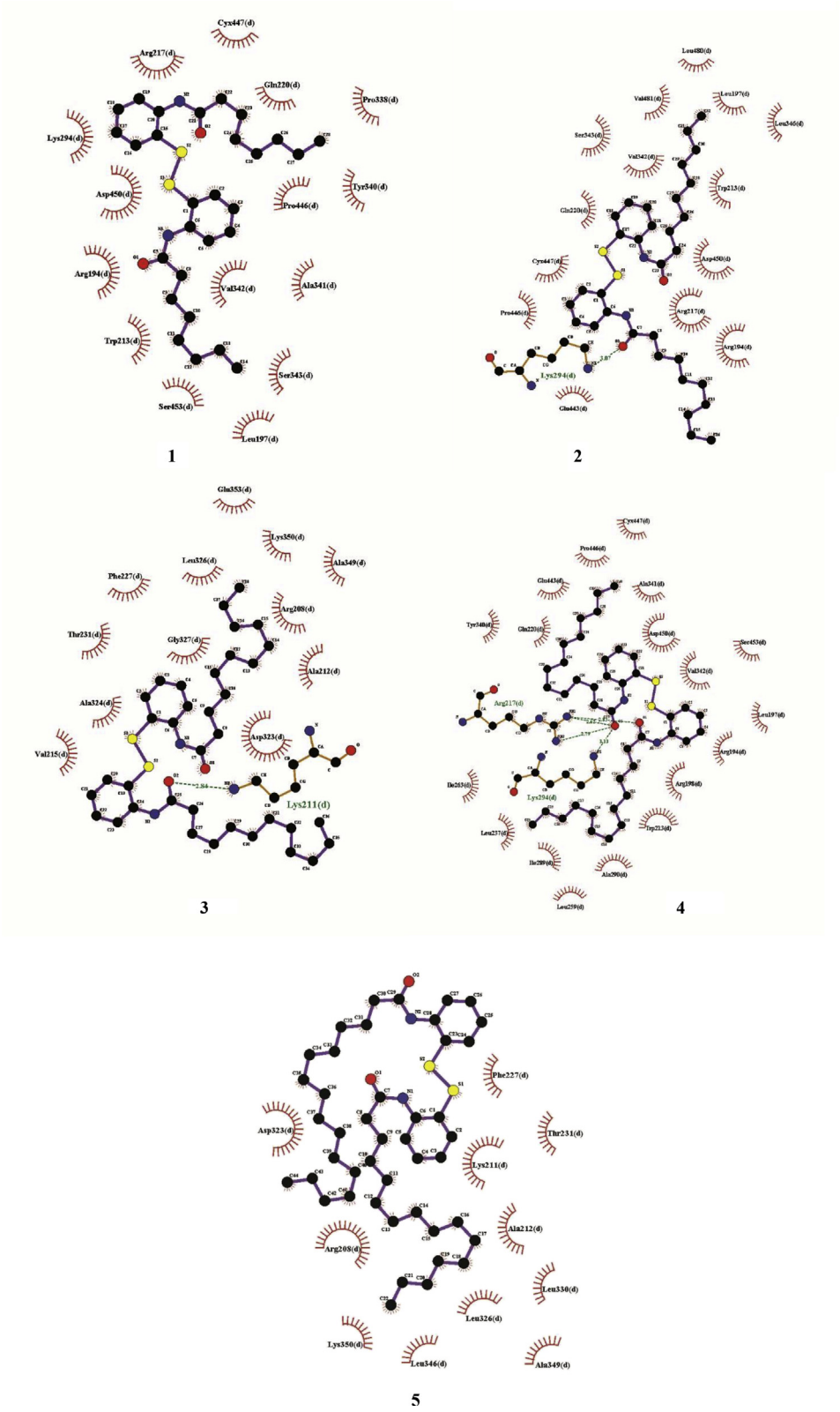

Figure 4. Interaction diagrams for docking of 1–5 in the vicinity of Trp-213.

$$\frac{A_{Compound}}{A_{Blank}} \times 100 \quad (7)$$

It was found that an increase in chain length (C_8-C_{14}) resulted in a decrease in the toxicity of the compounds towards HaCaT cells. The results also confirm that 1 is toxic to the cells at a concentration of <10 mg/ml while 2, 3 and 4 are non-toxic at the same concentration.

3. Experimental section

Thionyl chloride (99.5%) was obtained from Fluka chemical. Tetrahydrofuran (THF) (99.9%), dichloromethane (DCM) (99.9%) and triethylamine (99.5%) from Sigma-Aldrich. Melting points were measured on a Fischerbrand digital melting point apparatus. Infrared spectra were

Table 6. MIC values for compounds 1-5.

	MIC (mM)				
	1	2	3	5	+ve control
Gram-positive					
S.aureus (ATCC 29213)	12.5	5.40	2.50	>10.0	0.0152
B.cereus (ATCC 10876)	3.12	2.53	10.0	>12.5	0.0123
Gram-negative					
E. coli (ATCC 22922)	21.4	>25.3	>36.5	56.3	0.686
K. pneumonia (ATCC 13883)	25.3	26.3	28.9	50.2	0.0107
P. aeruginosa (ATCC 27853)	>15.6	25.6	>35.6	>46.5	0.171

+ve control: CTAB.

recorded on a Brucker Alpha FTIR spectrometer. ^{1}H NMR, ^{13}C NMR, DEPT, ^{1}H-^{1}H COSY and ^{1}H-^{13}C HMBC were recorded using a Bruker spectra spin NMR spectrometer at 250 MHz for ^{1}H NMR and 62.9 MHz for ^{13}C NMR in $CDCl_3$ as solvent. Fluorescence spectrophotometry were performed using a Perkin-Elmer LS-55 spectrophotometer. Elemental analysis was performed using a Eurovector EA3000 (CHNS) elemental analyser.

3.1. Synthesis of compound 1-5

An excess of thionyl chloride was added to a dissolved solution of fatty acid (octanoic, decanoic, dodecanoic, myristic and palmitic acid) in dichloromethane (25 mL) and was refluxed for 3 h. The solvent and any unreacted thionyl chloride were then removed via simple distillation. The corresponding acid chlorides obtained were added to a stirred solution of 2-amino phenyl disulfide in tetrahydrofuran (40 mL) and triethylamine (2.0 mL) and was refluxed for 3 h. The reaction was quenched with 15 mL of distilled water. The organic layer was then extracted using ethyl acetate (3 × 15 mL). The combined organic extracts were dried over anhydrous $MgSO_4$ and filtered. The solvent was then removed under reduced pressure. The crude residue was washed with methanol to remove any insoluble impurities followed by recrystallized in ethanol.

Dioctyl 2,2′-disulfanediyldibenzamide, 1. White powder. Yield: 29%; mp 57-59 °C [Found: C, 67.62% H, 9.13% N, 5.69% S, 11.86%; required $C_{28}H_{40}S_2N_2O_2$ C, 67.20%; H, 8.00%; N, 5.60%; S, 12.8%]; IR: (ν_{max}/cm^{-1}) 465 (S-S), 1655 (C=O), 3269 (-NH).

Didecanoyl 2,2′-disulfanediyldibenzamide, 2. White powder. Yield: 51.1%; mp 77-83 °C; [Found: C, 69.81%; H, 10.88%; N, 6.57% S,

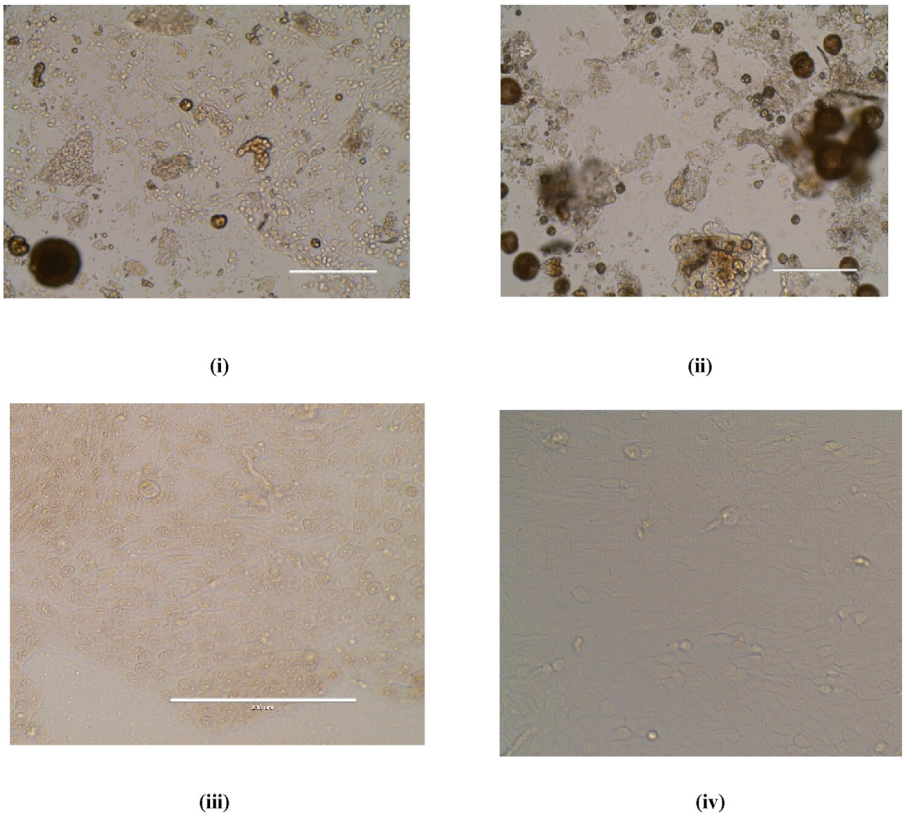

Figure 5. HaCaT cells treated with (i) 10 mg/ml of disulfide 1, (ii) 10 mg/ml of disulfide 3, (iii) 20% DMSO (positive control) and (iv) 4% ethyl acetate (negative control).

Table 7. % Cell viability in the presence of varying concentration of disulfides 1 to 4.

Concentration/(mg/ml)	% Cell Viability			
	1	2	3	4
20	18.4	-	100.0	100.0
10	23.0	63.7	100.0	100.0
5	62.6	100.0	100.0	100.0
2.5	82.9	100.0	92.1	100.0

11.40%; required $C_{32}H_{48}S_2N_2O_2$ C, 69.06%; H, 8.63%; N, 5.00%; S 11.51%]; IR: (ν_{max}/cm^{-1}) 463 (S-S), 1659 (C=O), 3267 (-NH).

Didodecanoyl 2,2′-disulfanediylbenzamide, 3. White powder. Yield, 67%; mp: 87–94 °C; [Found: C, 70.67%; H, 9.43%; N, 5.00%; S, 10.01%; required $C_{36}H_{40}S_2N_2O_2$ C, 70.59%; H, 6.54%; N 4.58%; S 10.46%]; IR: (ν_{max}/cm^{-1}) 465 (S-S), 1656 (C=O), 3267 (-NH).

Dimyristoyl 2,2′-disulfanediylbenzamide, 4. White powder; Yield, 61.4%; mp: 94–98 °C; [Found: C, 73.02%; H, 9.06%; N, 3.85%; S, 9.56% required $C_{44}H_{72}N_2S_2O_2$ C, 72.88%; H, 10.01%; N, 3.86%; S, 8.84%]; IR: (ν_{max}/cm^{-1}) 454 (S-S), 1658 (C=O), 3278 (-NH).

Dipalmitoyl 2,2′-disulfanediylbenzamide, 5. White powder. Yield, 63%. IR: (ν_{max}/cm^{-1}) 454 (S-S), 1658 (C=O), 3278 (-NH).

3.2. Antibacterial activity

Antibacterial tests were carried out against 2 Gram-positive (*Staphylococcus aureus* (ATCC 29213) and *Bacillus cereus* (ATCC 10876)) and 3 Gram-negative strains (*Escherichia coli* (ATCC 22922), *Klebsiella pneumonia* (ATCC 13883) and *Pseudomonas aeruginosa*) using the broth-dilution method in 96-well plates as described in our previously reported method [24]. The concentration of the compounds used were in the range of 10–100 mM. Cetyltrimethylammonium bromide (CTAB) and DMSO were used as positive and negative control respectively. The antibacterial activities were expressed in terms of their minimum inhibitory concentration (MIC).

3.3. In-vitro cytotoxicity assay

HaCaT cells in 100 μL of medium (Dulbecco's Modified Eagle Medium (DMEM) supplemented with 50 mL fetal bovine serum (FBS), 5 mL N-glutamine, 5 mL Streptomycin and penicillin) were seeded in 96-well plates one day prior to the experiment and left to incubate for 24 h. After incubation the medium was removed and the cells were treated with the disulfifes **1 to 5** (20–1.25 mg/mL). The cells were also treated with the blank solution (4% ethyl acetate) and the positive control (20% DMSO) and incubated at 37 °C at 5% CO_2 for 24 h. Following incubation, the cells were evaluated for any changes in morphology using An Evos FL Auto cell-imaging high-resolution microscope. The medium was removed and the cells were washed with phosphate-buffered saline solution (PBS) (100 μL). MTT solution (50 μL, 1 mg/mL) were added to each well and the plates were incubated at 37 °C at 5% CO2 for further 2 h. After incubation, the MTT reagent was removed and isopropanol (100 μL) was added to each well. The 96-well plates were then swayed for 30 min at room temperature and the absorbance was recorded using a 141003F Synergy HTX multi-mode reader. Mean values of 3 wells per treatment were determined for at least 3 independent experiments.

3.4. BSA binding studies

All measurements were carried out on a Perkin-Elmer LS-55 spectrofluorometer equipped with a Xenon lamp, using a 1.0 cm quartz cuvette. The Perkin-Elmer FLWinlab software was used to calculate the wavelength values.

3.4.1. Steady state/intrinsic fluorescence study

BSA stock solution (10 μM) was prepared in phosphate buffer of pH 7.4. Phosphate buffer (2.0 mL, pH 7.4) and BSA stock solution (1.0 mL, 10 μM) were added to a quartz cuvette. The fluorescence intensity was read at 336 nm (excited at 295 nm) in the range of 300–400 nm at 298 K. The excitation slit and emission slit were set to 10 nm and 5.0 nm respectively. The BSA solution was then titrated with stock solution of the disulfides (0.001 M). The fluorescence of BSA for each addition was then read at 336 nm.

3.4.2. Thermodynamic BSA studies

Phosphate buffer (2.0 mL, pH 7.4) and BSA solution (1.0 mL, 10 μM) were added to a 1.0 cm quartz cuvette. The solution was excited at 295 nm and scanned in the range of 300–400 nm at 3 different temperatures namely: 298, 308 and 313 K. The BSA solution was then titrated against 15 μL of the disulfide.

3.4.3. Competitive binding studies of disulfides ***1 to 5*** using site markers

Phosphate buffer (1.5 mL, pH 7.4), site marker (warfarin or ibuprofen) (0.5 mL, 10 μM) and BSA (0.5 mL, 10 μM) were added to a 1.0 cm quartz cuvette. The BSA solutions were excited at 295 nm and scanned in the range of 300–400 nm at 298 K. The excitation and emission slits were set to 50 nm and 2.5 nm respectively. The BSA solutions were then titrated by successive addition of 1 μL of compound. A final volume of 15 μL of the disulfides were added. The fluorescence of the BSA solutions were then read at 336 nm. The same procedure was used for titration with ibuprofen site marker.

3.5. Critical micelle concentration (CMC)

CMC of disulfides 1-5 was evaluated at 298 K using pyrene as fluorescence probe in the concentration range of 10–5 mM. Pyrene stock solution (10 μL, 0.1 mM) was transferred into 20 different vials. After evaporation of the methanol, solutions of the disulfides 1-5 (3 mL) of varying concentrations were added to the vials to yield a final concentration of 1.6 μM of pyrene in each vial. The solutions in each vial were mixed mechanically using an orbital shaker for 24 h prior to recoding the spectra over the range of 350–450 nm. The excitation wavelength was set at 334 nm and the emission wavelength was recorded at 373 (I_1) nm and 384 (I_3) nm. The excitation and emission slits were set to 5.0 nm and 2.5 nm respectively. The CMC of the disulfides 1-5 were obtained from the graph of (I_1/I_3) against concentration of disulfide.

3.6. Molecular docking

The crystal structure of BSA was obtained from the Protein Data Bank (PDB, id: 4F5S) and hydrogen atoms were added using the Reduce package [25]. Gasteiger–Marsili charges [26] were then assigned to the BSA molecule using Open Babel 2.3.90 [27]. The BSA molecule together with the structures of the disulfides 1-5 (drawn and optimised using Avogadro 1.2.0 software) were imported into AutoDockTools and docking was subsequently done using the Autodock 4.2 software [28]. Docking was done inside a three-dimensional grid box of size (70 × 70 × 70) Å, with a grid spacing of 0.375 Å, centered on the Trp-213 or Trp- 134 residues to generate 100 low energy conformations using Lamarckian

genetic algorithm (GA). Interaction diagrams were made with LigPlot+ [29].

4. Conclusion

Diaryl disulfide derivatives with varying alkyl chain length (C_8-C_{16}) were found to possess interesting physicochemical properties and biological activities such as antibacterial activities and a relatively favourable interaction with blood protein. The binding abilities of the derivatives with BSA increase in chain length up to C_{12} and then decrease with further increase in chain length, exhibiting a cut-off at C_{12}. Investigation of the thermodynamic parameters showed that binding of the derivatives to BSA occurs mainly due to van der Waals' forces and hydrogen bonding. Molecular docking studies showed a similar trend to what was observed in the fluorescence binding studies and in most cases, the binding was found to be spontaneous and the disulfides showed greater binding affinity to the Trp 213 over the Trp 134 residue. The antibacterial activities of the derivatives against *Staphylococcus aureus* were found to increase from C_8 to C_{12} and then decrease at C_{16}, displaying a cut-off point at chain C_{12}. The C_{10} exhibited the highest inhibitory activity against *Bacillus cereus* with an MIC value of 2.53 mM. The cytotoxicity of the compounds evaluated against the human keratinocyte (HaCaT) cell line revealed that the toxicity towards the HaCaT cells decreased with increasing chain length. This study has shown that the diaryl disulfide derivatives can be promising candidate in the pharmaceutical industry due to their antibacterial activity. Furthermore, their ability to form micellar structures and their binding ability to blood protein together with a low toxicity profile are some of the main attributes of the compounds that make them suitable to be further investigated as drug carriers.

Declarations

Author contribution statement

Nausheen Joondan, Thessa Innasee: Conceived and designed the experiments; Performed the experiments; Analyzed and interpreted the data; Wrote the paper.

Sabina Jhaumeer Laulloo, Minu Bhowon: Analyzed and interpreted the data; Contributed reagents, materials, analysis tools or data; Wrote the paper.

Funding statement

This research was supported by grants from the Higher Education Commission (HEC), Mauritius.

Declaration of interest statement

The authors declare no conflict of interest.

Additional information

Supplementary content related to this article has been published online at https://doi.org/10.1016/j.heliyon.2020.e05368.

References

[1] G.W. Bemis, M.A. Murcko, The properties of known drugs. 1. Molecular frameworks, J. Med. Chem. 39 (1996) 2887–2893.

[2] M.E. Welsch, S.A. Snyder, B.R. Stockwell, Privileged scaffolds for library design and drug discovery, Curr. Opin. Chem. Biol. 14 (2010) 347–361.

[3] R.D. Taylor, M. MacCoss, A.D. Lawson, Combining molecular scaffolds from FDA approved drugs: application to drug discovery, J. Med. Chem. 60 (2017) 1638–1647.

[4] M. Aldeghi, S. Malhotra, D.L. Selwood, A.W. Chan, Two and three-dimensional rings in drugs, Chem. Biol. Drug Des. 83 (2014) 450–461.

[5] (a) Z. Xu, P. Li, W. Qiao, Z. Li, L. Cheng, Effect of aromatic ring in the alkyl chain on surface properties of arylalkyl surfactant solutions, J. Surfactants Deterg. 9 (3) (2006) 245–248;
(b) Z. Xu, D. Liu, W. Qiao, Z. Li, Cheng, L. Synthesis and surface active properties of novel nonionic aryl oleic diethanolamide surfactants, Petrol. Sci. Technol. 24 (11) (2006) 1363–1370.

[6] R. Bordes, J. Tropsch, K. Holmberg, Role of an amide bond for self-assembly of surfactants, Langmuir 26 (2010) 3077–3083.

[7] R. Tan, P. Jensen, P. Williams, W. Fenical, Isolation and structure assignments of Rostratins A−D, cytotoxic disulfides produced by the marine-derived fungus Exserohilumrostratum, J. Nat. Prod. 67 (8) (2004) 1374–1382.

[8] D. Scharf, A. Habel, T. Heinekamp, A. Brakhage, C. Hertweck, Opposed effects of eEnzymatic gliotoxin N- and S-methylations, J. Am. Chem. Soc. 136 (33) (2014) 11674–11679.

[9] R. Davis, I. Sandoval, G. Concepcion, R. Moreira da Rocha, C. Ireland, Lissoclinotoxins E and F, novel cytotoxic alkaloids from a philippine didemnid ascidian, Tetrahedron 59 (16) (2003) 2855–2859.

[10] M. Góngora-Benítez, J. Tulla-Puche, F. Albericio, Multifaceted roles of disulfide bonds. peptides as therapeutics, Chem. Rev. 114 (2) (2013) 901–926.

[11] Y. Yao, Z. Tu, C. Liao, Z. Wang, S. Li, H. Yao, Z. Li, S. Jiang, Discovery of novel class I histone deacetylase inhibitors with promising in vitro and in vivo antitumor activities, J. Med. Chem. 58 (19) (2015) 7672–7680.

[12] L. Brülisauer, M. Gauthier, J. Leroux, Disulfide-containing parenteral delivery systems and their redox-biological fate, J. Contr. Release 195 (2014) 147–154.

[13] D. Yang, W. Chen, J. Hu, Design of controlled drug delivery system based on disulfide cleavage trigger, J. Phys. Chem. B 118 (43) (2014) 12311–12317.

[14] S. Durmus, A. Dalmaz, E. Calıskan, G. Dulger, Synthesis and characterization of disulfide-Schiff base derivatives and in vitro investigation of their antibacterial activity against multidrug-resistant acinetobacter baumannii isolates: a New Study, Russ. J. Gen. Chem. 88 (2) (2018) 305–311.

[15] S. Oliveira, Z. Kleber, C. Andrade, R. Varela, J. Molinillo, F. Macías, Phytotoxicity study of ortho-disubstituted disulfides and their acyl derivatives, ACS Omega 4 (1) (2019) 2362–2368.

[16] T. Schmid, J. Blees, M. Bajer, J. Wild, L. Pescatori, G. Cuzzucoli Crucitti, L. Scipione, R. Costi, C. Henrich, B. Brüne, N. Colburn, R. Di Santo, Diaryl disulfides as novel stabilizers of tumor suppressor Pdcd4, PloS One 11 (3) (2016), e0151643.

[17] Z. Vinarov, V. Katev, D. Radeva, S. Tcholakova, N. Denkov, Micellar solubilization of poorly water-soluble drugs: effect of surfactant and solubilizate molecular structure, Drug Dev. Ind. Pharm. 44 (4) (2017) 677–686.

[18] H.B. Klevens, Structure and aggregation in dilute solutions of surface active agents, J. Am. Oil Chem. Soc. (1953) 74–80.

[19] Q. Jiao, R. Wang, Y. Jiang, B. Liu, Study on the interaction between active components from traditional Chinese medicine and plasma proteins, Chem. Cent. J. 12 (1) (2018).

[20] A. Valstar, M. Almgren, W. Brown, M. Vasilescu, The interaction of bovine serum albumin with surfactants studied by light scattering, Langmuir 16 (2000) 922–927.

[21] Y. Wang, X. Jiang, L. Zhou, L. Yang, G. Xia, Z. Chen, M. Duan, Synthesis and binding with BSA of a new gemini surfactant, Colloid. Surface. Physicochem. Eng. Aspect. 436 (2013) 1159–1169.

[22] D. Smith, L. Di, E. Kerns, The effect of plasma protein binding on in vivo efficacy: misconceptions in drug discovery, Nat. Rev. Drug Discov. 9 (12) (2010) 929–939.

[23] S. Ghosh, J. Dey, Binding of fatty acid amide amphiphiles to bovine serum albumin: role of amide hydrogen bonding, J. Phys. Chem. B 119 (25) (2015) 7804–7815.

[24] N. Joondan, P. Caumul, S. Jhaumeer-Laulloo, Investigation of the physicochemical and biological properties of proline-based surfactants in single and mixed surfactant systems, J. Surfactants Deterg. 20 (1) (2016) 103–115.

[25] J.M. Word, S.C. Lovell, J.S. Richardson, D.C. Richardson, Asparagine and glutamine : using hydrogen atom contacts in the choice of side-chain amide orientation, J. Mol. Biol. 285 (1999) 1735–1747.

[26] J. Gasteiger, M. Marsili, A new model for calculating atomic charges in molecules, Tetrahedron Lett. 19 (1978) 3181–3184.

[27] N.M. O'Boyle, M. Banck, C.A. James, C. Morley, T. Vandermeersch, G.R. Hutchison, OpenBabel : an open chemical toolbox, J. Cheminf. 3 (2011) 1–14.

[28] G.M. Morris, R. Huey, W. Lindstrom, M.F. Sanner, R.K. Belew, D.S. Goodsell, A.J. Olson, AutoDock 4 and AutoDockTools4: automated docking with selective receptor flexibility, J. Comput. Chem. 30 (2009) 2785–2791.

[29] R.A. Laskowski, M.B. Swindells, LigPlot+: multiple ligand–protein interaction diagrams for drug discovery, J. Chem. Inf. Model 51 (2011) 2778–2786.